Accurate Thickness Measurements in Thin Films with Surface Analysis

M. P. Seah*,

Quality of Life Division, National Physical Laboratory, Teddington, Middlesex TW11 0LW, UK

*martin.seah@npl.co.uk

Received 4 October 2004; Accepted 14 January 2005

Quantification in surface analysis using Auger electron spectroscopy and X-ray photoelectron spectroscopy has been the topic of significant work at NPL. A new approach to the quantification of materials that are homogeneous over the analysis volume has been developed using new average matrix relative sensitivity factors. These show agreement between theory and experiment at ~10% for all peaks and elements analysed. For samples that are not homogeneous, layer thicknesses are often required. For ultra-thin gate oxides, the International Technology Roadmap for Semiconductors requires 1.3% accuracy. For this purpose, angle-resolved XPS is a good candidate. In a wide study under the auspices of the Consultative Committee for Amount of Substance (CCQM), the accuracy of measurements of the thicknesses of SiO_2 layers <8 nm thick on Si have been assessed. This study involved 45 sets of measurements in laboratories using MEIS, NRA, RBS, EBS, XPS, SIMS, ellipsometry, GIXRR, NR and TEM. The relative strengths and weaknesses become clear. These show that if XPS is used under reference conditions it can be reliable and fast with an accuracy, based on a calibration from the study, ~ 1%. Inter-method correlations as good as 0.05 nm are achieved over the 8 nm range. Furthermore, certain methods, thought to be accurate, suffer from incompleteness of the measurement method. For thicker layers, sputtering is generally used. Here a new method has been tested to generate a sputter yield database, for argon ions, of 26 critical elements. This database has been used to help evaluate a new semi-empirical theory of sputtering yields that includes terms missing from the current semi-empirical theories and removes errors that are up to, and may exceed, a factor of 5. The new theory agrees with published data at ~ 10% and shows why certain elements have anomalously high yields.

INTRODUCTION

Auger electron spectroscopy (AES) and X-ray photoelectron spectroscopy (XPS) are precise methods with excellent repeatability, however, high accuracy generally remains elusive. Here, we review improvements in accuracy in two complementary areas addressing composition depth profiling. Methods fall into two distinct classes: i) those where the profile is deduced non-destructively from the spectra and ii) those involving ion sputtering where surface signals are followed as a function of the sputtering time.

The first class can be excellent in the regime <8 nm where the second has more difficulties. In the early stage of sputtering, contaminants are removed, the preferential sputtering of one element over another is changing, the bombarding ion is being implanted and the surface is being amorphised. This non-equilibrium stage can have a sputtering rate significantly higher than that at equilibrium and leads to uncertainty in the initial part of the profile, where the first class of methods is good. We shall illustrate both classes of measurement.

In the first area, the system of thermal SiO_2 on Si has been chosen. Oxide formed by other routes may give significantly different results. The International Technology Roadmap for Semiconductors (ITRS) [1] indicates a need for measurement of ultra-thin gate oxides at a standard uncertainty of 1.3%. In the analysis of thin layers by XPS there is a dominant

uncertainty of around 17.4% [2], arising from the inelastic mean free path (IMFP). However, analyses of thickness determinations by XPS show that the linearity of simple equations can be valid for 0.5 nm to 8 nm to within ± 0.025 nm[3]. In addition to XPS are the ion methods of medium energy ion scattering spectrometry (MEIS), Rutherford backscattering spectrometry (RBS) and elastic backscattering spectrometry (EBS), which may also reach uncertainties as low as 2%. MEIS, RBS and EBS cover a much greater thickness range and have higher general accuracy than XPS. Additionally, there are layer thickness measuring methods using interference effects, that should also reach around 2% but do not have analytical power. Here we shall report a recent intercomparison of these and other methods under the auspices of CCQM [4].

The oxide is a uniform layer of thermal SiO_2, with each sample being between 1.5 and 8 nm thick on (100) or (111) Si wafer substrates the whole being covered by hydrocarbon contamination after manufacture. At the interface between the oxide and the substrate there will be suboxides simply because the interfacial layer of the substrate Si atoms in contact with the oxide have an environment that contains oxygen from the SiO_2 layer.

The analytical methods employed in this study were those listed above and nuclear reaction analysis (NRA). The methods that give length are grazing incidence X-ray reflectometry (GIXRR), neutron reflectometry (NR) and transmission electron microscopy (TEM). These are all vacuum methods. Other methods using optics are ellipsometry and spectroscopic ellipsometry (SE) which are conducted in the air. The amount of SiO_2 on Si measured by methods that give the amount of substance, is related to the layer thickness by the SiO_2 density. Here, the value 2.196 g cm^{-3} is used. This density is consistent with reported values for thermal oxides [5].

In the second area, we have developed new, higher accuracy, general equations for predicting sputtering yields for elements using inert gas ions and have tested them with measurements on nano-craters. The existing generic equations have errors of 20% for some elements and 50% for others, reaching a factor of 5 in the worst case. This uncertainty has been reduced, by inclusion of a new term, to 10% when compared with published experimental data. The new method is rapid and allows new effects to be observed.

PREPARATION OF THE SAMPLES

For the thermal SiO_2 on Si samples, all material was grown by thermal oxidation in furnaces designed for ultra-thin gate oxides. The wafers were mapped for the oxide uniformity by ellipsometry, with a precision around 0.002 nm, allowing samples to be selected from regions of the wafers that were homogeneous to 1% [6]. The cleaned samples were then shipped in polypropylene “Fluoroware” which would typically keep the carbonaceous contamination below 0.25 nm for 3 months [7]. Repeat XPS measurements showed the oxides to be very stable. Those returning XPS data early were invited to repeat the measurements using a reference geometry (RG) explained below [6].

For the nano-craters, 26 solid elements were polished with 1 μm diamond paste. These were then sputtered with a 10 μm focused 5 keV argon ion beam at 45° incidence angle to form craters, typically, <1 μm deep. The volumes of these craters were measured, after air exposure, using a Park Autoprobe CP AFM. Measurements for 3 craters for each sample showed a repeatability of 7%.

RESULTS AND DISCUSSION

Thickness from XPS

Method for Evaluating the Results

The thicknesses of each uniform wafer were measured by XPS at NPL using the RG which was 34° from the surface normal in an azimuth at 22.5° to one of the edges of the square (100) samples or at 25.5° from the surface normal in an azimuth of one of the edges of the triangular (111) samples. Details of the method are given by Seah and Spencer [6]. Briefly, from the Si 2p spectra, the X-ray satellites were removed together with the $2p_{3/2,1/2}$ spin-orbit splitting determined as 50% of the intensity at 0.60 eV higher binding energy [8]. The remaining structure was evaluated as 5 peak intensities, I_{Si}, I_{Si2O} at 0.95 eV higher binding energy (BE), I_{SiO} at 1.75 eV higher BE, I_{Si2O3} at 2.48 eV higher BE and I_{SiO2} at

3.8 to 4.3 eV higher BE, as defined by Hollinger and Himpsel [8] and by Keister *et al* [9]. The thickness of the oxide may be calculated using the well-known relation for photoelectrons from the metal and oxide states of a single peak.

$$d = L\cos\theta \ln(1 + R_{expt} / R_o) \qquad (1)$$

where d is the oxide thickness, L is the attenuation length of both the substrate and oxide photoelectrons in the oxide, R_{expt} is the ratio of the measured intensities of the photoelectrons from the oxide and the elemental states from the sample, and R_o is the ratio of these intensities from bulk materials. To allow for the intermediate oxides, we replace Eq (1) by four separate equations, one for each suboxide [3]. The effective oxide thickness, d_{oxide}, is then given by the sum [5]: $d_{oxide} = d_{SiO2} + 0.75d_{Si2O3} + 0.5d_{SiO} + 0.25d_{Si2O}$ which apportions the thickness according to the oxygen content. From measurements elsewhere [3], R_o is 0.9329. Calculations of L are given by Seah and Spencer [6], based on the IMFP value of Tanuma, Powell and Penn [10], thought to be accurate to 17.4% [2]. For all the samples, the difference between d_{oxide} and d_{SiO2}, as measured, is 0.128 ± 0.008 nm, equivalent to a simple match of SiO_2 and Si at a flat interface.

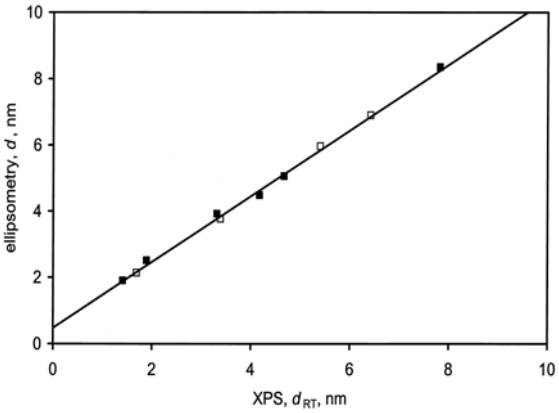

Fig. 1 Correlation plot for ellipsometry from NPL with the NPL XPS reference values, ■ (100) and □ (111) surfaces, after Seah *et al*[5]. The least squares line gives the gradient, *m*, and the intercept or offset *c*. The rms scatter of the results about the line, *r*, gives the combined repeatabilities of the two methods. The ellipsometry data are for samples soon after preparation and without removal from a dust-free environment between manufacture and measurement.

Here, all the uncertainties given are standard uncertainties.

The data returned to NPL for the thicknesses of the samples were then plotted against their reference thicknesses, d_{RT}, and the result fitted with a straight line of the following form, as shown in Fig. 1 [5]:

$$d_{respondee} = md_{RT} + c \qquad (2)$$

In addition to *m* and *c*, we also evaluate *r*, the rms scatter of the data about the straight line fit. Figure 1 shows the correlation of the ellipsometry data used for mapping the wafers and d_{RT}. There is no significant difference between (100) and (111) samples. This plot gives a gradient *m* of 0.993 ± 0.016, an offset *c* of 0.480 ± 0.070 nm and an rms scatter, *r*, of 0.089 nm. The offset *c*, arises from the ellipsometry detecting layers of water and carbonaceous contamination equivalent to 0.480 nm of oxide.

The Results

MEIS is a well-established technique for measuring thin film quantities. Two laboratories provided MEIS data, the Korean Research Institute of Standards and Science (KRISS) and Daresbury Laboratory. Both used proton beams ~100 keV, incident and emitted along channelling directions to reduce the background and improve the measurement statistics. Both before and after scattering, the protons lose energy at a rate defined by their energy and the material. These rates are available from SRIM 2003 [11] with estimated accuracy of 4%. Two peaks are seen in the spectrum, the first at around 90% of the beam energy is for Si, and the second at around 82% is for O. From the energy loss, the thickness of the oxide layer is determined. The oxygen width is a measure of the thickness of all O containing material. This will be the SiO_2, the intermediate oxides and O in contamination such as water. This leads to an average $m = 0.953 \pm 0.040$ and $c = 0.483 \pm 0.108$ nm. The results for the Si peak give an extra value for *m*. The results for KRISS and Daresbury are given later in Fig. 3. The average and standard deviation of the *m* and *c* values for MEIS are given in Table 1.

NRA, like MEIS, allows the total oxygen content in a film to be measured. Here, an 860 keV deuteron beam is used to strike ^{16}O atoms causing protons to be detected from the $^{16}O(d,p_1)^{17}O^*$ reaction [12]. To calibrate NRA, a reference sample is produced by anodic oxidation with a known number of oxygen atoms m^{-2}. Quantities are then derived from the counting ratios for the reference and the unknown film. The NRA results are shown in Table 1 and give $m = 1.074 \pm 0.034$ with the uncertainty coming from both the reference film and the data fitting. The offset of 0.480 nm is similar to the offsets seen in MEIS and also arises from the oxygen contamination.

RBS and EBS have many of the attributes of MEIS but work at higher beam energies. These allow thicker films to be measured but the poor energy resolution does not permit the thickness to be measured from the peak width. Instead, the peak intensities are used. RBS studies have been completed in The Netherlands and in Singapore whereas EBS is conducted in Germany and the UK. In these studies a single alignment mode is used.

In the National University of Singapore (NUS), a 2 MeV He^+ ion beam is used. The oxygen signal, Y, is then related to the thickness, d, via the equation $Y = N\,d\,\sigma\,\Omega Q$ where N is the oxygen atomic density, σ is the Rutherford cross section with screening, Ω is the detector solid angle and Q the integrated charge from the beam. The results for the O peak give m = 1.072, c = 0.351 nm and r = 0.510 nm. The rather high scatter arises from the low peak intensity. The offset c arises for the same reasons as given for MEIS and NRA. In addition to the O data, Si thicknesses may be evaluated from the NUS measurements and give m = 0.927. Data from Philips gave m = 0.968, c = 0.506 nm and r = 0.286 nm.

The Universities of Jena and Surrey both used EBS with the non-Rutherford cross section for the $^{16}O(\alpha,\alpha)^{16}O$ resonance at 3036 keV with a ^4He beam. This enhances the cross section 20 times compared with the Rutherford cross section but now the cross section needs to be measured. From the University of Jena data we get m = 0.981, c = 0.463 nm and r = 0.253 nm. The University of Surrey data give m = 1.075, c = 0.950 nm and r = 0.168 nm for the O peak and m = 1.063 for the Si peak.

This completes the data for methods specifically analysing the oxygen content. Note that the average offsets of the O data are 0.483, 0.480 and 0.568 nm, respectively, averaging 0.510 ± 0.050 nm. This is equivalent to ~2 monolayers of adsorbed water. This is expected since there will be one monolayer of tightly bound chemisorbed water together with some additional water and oxygen in the adsorbed hydrocarbons.

Studies in XPS may be conducted in a number of ways. The method described above is the method used at NPL. If the spectra are recorded using unmonochromated X-rays, the X-ray satellites should first be removed. Next the spin orbit splitting of the Si 2p peak is deconvolved to leave just the $2p_{3/2}$ peak. Next, a Shirley background is removed. Finally, the peak structure may be analysed into the 5 peaks. Not all analysts used these procedures and this led to small variations in the m and c results.

Thirteen sets of XPS data have been received from the Bundesanstalt für Materialforschung und Prüfung (BAM), the National Research Council of Canada, the National Metrology Institute of Japan (NMIJ), the University of Utsunomiya, NTT, the National Institute for Materials Science, the PSB Corporation, NUS, the Institute of Materials Research & Engineering, CSIR - National Metrology Laboratory of South Africa, the Swiss Federal Laboratories for Materials Testing and Research, NPL and Philips using a variety of instruments, procedures and calculational routes. The scatter of the open symbols in Fig 2 reflects these variations and the problems of forward focusing [6] associated with detection along low index directions. The use of the RG avoids this. Eleven sets of data were received using the RG and these, using R_o and L as given earlier, leads to the dramatic improvement shown in Fig. 2, to $m = 1.001 \pm 0.026$ and $c = -0.013 \pm 0.110$ nm.

Ellipsometry is a fast and precise method for thin film measurement. Some laboratories used one measure at the HeNe laser wavelength of 632.8 nm and others used spectroscopic ellipsometry over the wavelength range, typically, $200 < \lambda < 850$ nm.

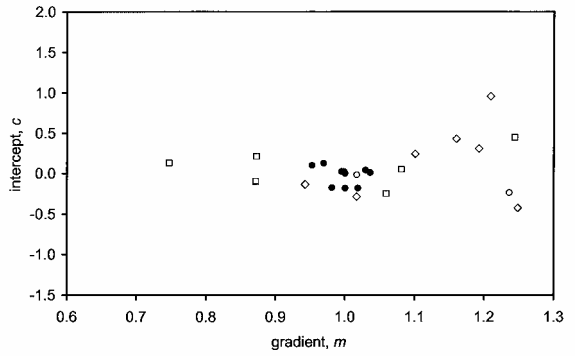

Fig. 2 Plot of m and c for the XPS thickness data as reported, (□) using 0° emission, (◊) using ARXPS and fitting $\ln(1 + R_{expt}/R_o)$ versus θ to determine d, (O) single emission angles, and (●) for the RG using R_o = 0.9329, L(Mg) = 2.964 nm and L(Al) = 3.448 nm, after Seah *et al*[5].

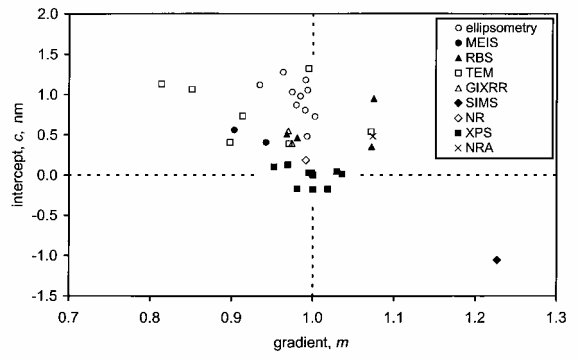

Fig. 3 Plots of m and c for the homogenised data and, for XPS, for the RG[5]. Any corrections used for surface contaminations by individual laboratories are not included here. This shows the direct result of applying each method.

Briefly, an ellipsometer measures the change in the phase difference between the parallel and perpendicular components of specularly reflected light and the ratios of the outgoing wave amplitudes to the incoming wave amplitudes for these components. From these and the known optical constants, the film thickness can be measured. However, it is not easy to quantify the effects of the contamination.

Here, data have been received from the Physikalisch-Technische Bundesanstalt (PTB), BAM, NTT, the University of Leipzig, NPL and the National Institute of Standards and Technology (NIST). All of the data sets gave excellent linearity with an average r value <0.1 nm. The precision here is excellent and the values of m give $m = 0.986 \pm 0.011$. The fits of the data for spectroscopic ellipsometry confirm that the material is consistent with the bulk thermal oxide. Using the 10 values as estimates of a true value of m gives the standard error of the mean as 0.004, as shown in Table 1. The m and c values for ellipsometry are shown in Fig. 3. The offset values, c, ranged from 0.480 nm to 1.276 nm. The former value was obtained directly after the wafers were made, whereas the average value was higher at 1.016 nm. This offset arises from both water and carbonaceous contaminations and is higher than for other methods since the data are acquired in air. The data from NIST also used a 3 minute pre-heat to 260° C which reduces the offset by 0.22 nm and stabilises the contamination

Whereas the analytical techniques provide the amount of substance, GIXRR and NR measure length and, d, is deduced via the relation $n\lambda = 2d\cos\theta$, where λ is the wavelength of the radiation. At PTB, GIXRR was conducted in UHV at BESSY II. At the beam energies usually used, around 8 keV, the contrast between SiO_2 and Si is poor. Contrast was enhanced by working at an energy just above the Si K absorption edge at 1841 eV [13] and wavelength 0.674 nm. Reflectance measurements for $81° < \theta < 90°$ lead to intensity oscillations from which the thickness may be deduced with high precision at 8 nm but poorer at 2 nm. In the second GIXRR study at NMIJ, a rotating anode diffractometer was used in air. The higher energy X-rays lead to poorer contrast and hence a need to model the intensities very carefully.

In the third of these interference studies, at NIST, neutron reflectometry (NR) is conducted as described by Dura *et al* [14] using neutrons of wavelength 0.475 nm. The behaviour is similar to GIXRR but, in general, NR gives superior contrast since, in the former, the scattering depends on the nuclear structure whereas, in the latter it is, to first order, proportional to atomic number Z. NR is thus less sensitive to the carbonaceous and water contaminations.

Table 1 - Average values of *m* and *c* by method in ascending *c* with the standard deviations and, bracketed, standard deviations of the means.

Method	*m*	*c*, nm
XPS RG	1.001 ± 0.026 (0.009)	-0.013 ± 0.110 (0.037)
NR[a]	0.991 ± 0.008 (0.008)	0.185 ± 0.050 (0.050)
NRA[a]	1.074 ± 0.034 (0.034)	0.480 ± 0.122 (0.122)
MEIS	0.953 ± 0.040 (0.020)	0.483 ± 0.108 (0.076)
GIXRR	0.972 ± 0.003 (0.002)	0.551 ± 0.004 (0.003)
RBS, EBS	1.014 ± 0.064 (0.026)	0.568 ± 0.263 (0.132)
TEM	0.915 ± 0.099 (0.035)	0.804 ± 0.361 (0.128)
Ellipsometry	0.986 ± 0.011 (0.004)	Pre-heat: 0.871 ± 0.092 (0.046)
		No pre-heat: 1.016 ± 0.174 (0.062)
[a] One result, standard deviation calculated from the fit for *m* and *c*.		

TEM studies, like GIXRR and NR provide a direct length measurement but here it is from the image of the cross section of the film in which the pitch of the Si atoms is a traceable calibrant. Sets of TEM data were received from PTB, BAM, Philips, KRISS, EMPA, Daresbury and Bell Laboratories using either high resolution conventional TEM (HRTEM) or scanning TEM with annular dark field detection (HAADF-STEM). In order to prepare samples, the surface needs capping. Ti, Al, Si, Au and epoxy were all used and gave adequate contrast. In all cases, the main issue was in defining the interface position. In general, the 50% intensity levels were used but these may not give the correct thickness. The results scattered very much more than expected, as shown by Fig. 3 and by the uncertainties in Table 1. There was no significant difference between the HRTEM and HAADF-STEM data.

The Sputtering Yields

The New Theory

Starting from the approaches of Matsunami *et al* [15] and Yamamura and Tawara [16], we have reassessed the published yield data for sputtering using krypton, argon and xenon ions [17,18]. The basic theory originates with Sigmund's equation[19] where the sputtering yield, *Y*, for an ion of energy, *E*, is given by:

$$Y = \frac{0.042\ Q\ \alpha^*}{U_o}\ \frac{S_n(E)}{1+A s_e(\varepsilon)}\ \left(1-\left(\frac{E_{th}}{E}\right)^{1/2}\right)^s \qquad (3)$$

where α^* is a dimensionless factor that provides the proportion of energy from the incident ion back-reflected to be available for sputtering, $S_n(E)$ is the nuclear stopping power per atom and $s_e(\varepsilon)$ is the inelastic electronic stopping at a reduced energy, ε. E_{th} is the threshold energy for sputtering and U_o the surface binding energy per atom. The parameters A and s differ for the above two approaches. In both approaches, the parameter Q is obtained by fitting to experimental data for each element and simply scales the whole yield. Q values are available for 34 elements but for other elements Q is set at unity. The uncertainty in the Qs for the 34 elements is 20% but for the other elements it is much higher, often exceeding a factor of 2[17]. We follow much of the analysis given by these authors, except for the evaluation of Q and α^*. In the above approaches, both follow Sigmund and assume that Q is a fixed number for each element and α^* is dependent only on the ratio M_2/M_1 where the subscript 1 applies to the incident ion and the 2 to the target atom.

In practice, it is clear that α^* depends on a product of terms in M_2/M_1, in M_1 and in properties of the target atoms so that the above analysis leads to large uncertainties. To stay close to the above approaches, we retain their α^* and simply make Q dependent on the target atoms and M_1. We can see the main effect by analysing all the major data sets for one incident ion, argon [17]. From the data for 28 elements we get new Q_{eff} values. The scatter of data about the predictions as a function of energy is 8.2%.

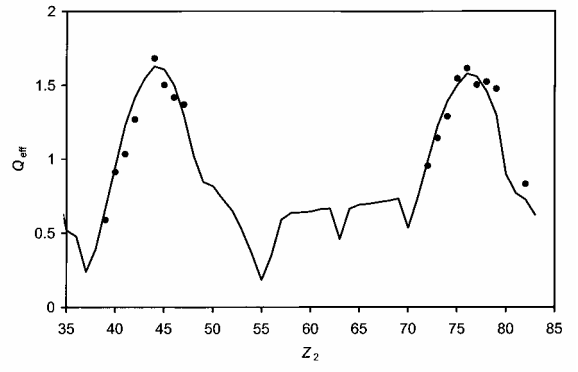

Fig. 4 Correlation of Q_{eff} (●) and $0.0221r^{-3}$ (—) using Matsunami *et al*'s [15] approach, after Seah *et al* [17].

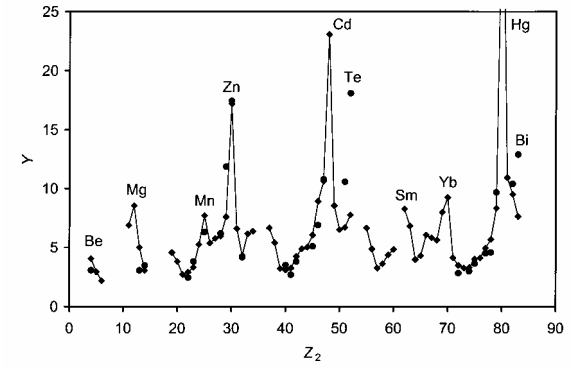

Fig. 5 The measured Y (●) and the predictive relations using Matsunami *et al*'s[15] approach with the new $f(M_1,M_2)$ for Q with Yamamura *et al*'s [20] angular dependence (◆), after Seah *et al* [17].

Figure 4 shows, over a limited range of the target atom atomic number, Z_2, the correlation of the new Q_{eff} and $0.0221r^{-3}$. This shows the essential correlation of Y with density that is omitted in one of Sigmund's approximations. Figure 4 is shown over this range since, for argon, $Q_{eff} = f(M_2)/r^3$, where $f(M_2)$ is slowly moving with M_2. A simple analytical equation can be derived for $f(M_2)$ that is better for Matsunami *et al*'s approach than that of Yamamura and Tawara [17]. This function is slightly different for neon and xenon and so we should write it as $f(M_1,M_2)$ [18].

We do not recommend our equation to be extended beyond inert gas incident ions since it does not allow for the need to sputter the implanted ions from the beam which would, for instance, be required for self sputtering or sputtering with metal ions. Argon typically accumulates to only 2.5% [18] and so may, exceptionally, be ignored. These issues are not addressed by Matsunami *et al* [15] and Yamamura and Tawara [16] who treat all ions equivalently.

The New Results

Measurements of the craters using the calibrated AFM were relatively straightforward and repeatable, leading directly to a value for Y using bulk densities. Figure 5 shows a comparison of the results and our modification of Matsunami *et al*'s theory based on the $f(M_1,M_2)$ deduced from published data. Since our measurements are at 45° incidence, the angular effect of Yamamura *et al* [20] has been included. In these 26 elements, Zn, Sb, Te and Bi are new with no earlier data to deduce Q. What we see in Fig. 5 is that whilst Zn is well described, the other 3 elements have higher yields than the values predicted. This arises since these have unusually low values of U_o for the emission of polyatomic clusters, Eq (3) being for monatomic sputtering.

SUMMARY OF RESULTS

For measuring thickness by XPS, using the RG and the above values for L and R_o, we find m = 1.001 ± 0.026 and c = -0.013 ± 0.110 nm, an excellent improvement on previous studies. The XPS data are unique in that, if the method is correctly used, the thickness extrapolates linearly to zero at zero SiO_2 thickness, irrespective of the contamination. The average of all of the ellipsometry data gave $m = 0.986 \pm 0.011$. The offsets, c, however reflect various contaminations. The other data that should be consistent analytically are MEIS, RBS, EBS and NRA which give the total oxygen content. Averaging the data from Table 1 gives m = 1.014 ± 0.061, $c = 0.510 \pm 0.050$ nm. This c value represents oxygen in the water and hydrocarbon layers. The interference methods of GIXRR and NR give average m values of 0.972 ± 0.003 and 0.991 ± 0.008, respectively. GIXRR, NR and ellipsometry all have excellent traceabilities. The results for these data are given in Fig. 3 and in Table 1. Using weightings based on reciprocal variances, m = 0.986 ± 0.004 for the homogenised data. This may be used to re-calibrate the XPS by scaling the values of L by 0.986 to give 2.923 nm for Mg X-rays and 3.400 nm for Al X-rays.

The above value of *m* may also be used, for example, to improve the accuracy of MEIS analysis through recalibration of the stopping powers.

For depth profiling of materials by inert gas ion sputtering, a new formulation is provided to calculate sputtering yields accurately. This is based on an extension of Matsunami *et al*'s work and provides a new accurate way of calculating the *Q* values for all elements. This is supported by new measurements on nano-craters by AFM. Elements such as Sb, Te and Bi, which have low binding energies for cluster emission, are shown to have anomalously high sputtering yields.

ACKNOWLEDGEMENTS

The author would like to thank the organisers of PSA-04 for inviting this review and S J Spencer and I S Gilmore for comments. This work is supported by the National Measurement Policy Unit of the UK Department of Trade and Industry.

REFERENCES

[1] *International Technology Roadmap for Semiconductors*, (2001 or 2002 editions) http://public.itrs.net/.

[2] C. J. Powell and A. Jablonski, *J. Phys. Chem. Ref. Data* **28**, 19 (1999).

[3] M. P. Seah and S J Spencer, *Surf. Interface Anal*. **35**, 515 (2003).

[4] *CCQM, Consultative Committee for Amount of Substance – Metrology in Chemistry*, www.bipm.fr/enus/2_Committees/CCQM.shtml.

[5] M. P. Seah, S. J. Spencer, F. Bensebaa, I. Vickridge, H. Danzebrink, M. Krumrey, T. Gross, W. Oesterle, E. Wendler, B. Rheinländer, Y. Azuma, I. Kojima, N. Suzuki, M. Suzuki, S. Tanuma, D. W. Moon, H. J. Lee, Hyun Mo Cho, H-Y. Chen, A. T. S. Wee, T. Osipowicz, J. S. Pan, W. A. Jordaan, R. Hauert, U. Klotz, C. van der Marel, M. Verheijen, Y. Tamminga, C. Jeynes, P. Bailey, S. Biswas, U. Falke, N. Nguyen, D. Chandler-Horowitz, J. R. Ehrstein, D. Muller and J. A. Dura, *Surf. Interface Anal*. **36**, 1269 (2004).

[6] M. P. Seah and S. J. Spencer, *Surf. Interface Anal*. **33**, 640 (2002).

[7] M. P. Seah and S. J. Spencer, *J. Vac. Sci. Technol*. A **21**, 345 (2003).

[8] G. Hollinger and F. J. Himpsel, *Appl. Phys. Lett*. **44**, 93 (1984).

[9] J. W. Keister, J. E. Rowe, J. J. Kolodziej, H. Nümi, H-S. Tao, T. E. Madey and G. Lucovsky, *J. Vac. Sci. Technol*. A**17**, 1250 (1999).

[10] S. Tanuma, C. J. Powell and D. R. Penn, *Surf. Interface Anal*. **17**, 927 (1991).

[11] J. F. Zeigler, *SRIM 2003.02 code IBM Yorktown Heights*, http://www.SRIM.org, SRIM-2003.

[12] G. Amsel, J. P. Nadai, C. Ortega, S. Rigo and J. Siejka, *Nucl. Ins. Meth*. **149**, 705 (1978).

[13] M. Krumrey, M. Hoffmann, G. Ulm, K. Hasche and P. Thomsen-Schmidt, *Proc. EVC 2003*, to be published.

[14] J. A. Dura, C. A. Richter, C. F. Majkrzak and N. V. Nguyen, *Appl. Phys. Lett*. **73**, 2131 (1998).

[15] N. Matsunami, Y. Yamamura, Y. Hikawa, N. Itoh, Y. Kazumata, S. Miyagawa, K. Morita, R. Shimizu and H. Tawara, *At. Data Nucl. Data Tables* **31** 1 (1984).

[16] Y. Yamamura and H. Tawara, *At. Data Nucl. Data Tables* **62** 149 (1996).

[17] M. P. Seah, C. A. Clifford, F. M. Green and I. S. Gilmore, *Surf. Interface Anal*. **37**, 444 (2005).

[18] M. P. Seah, *Nucl. Ins. Meth*. B, **229**, 348 (2005).

[19] P. Sigmund, *Phys. Rev*. **184** 383 (1969).

[20] Y. Yamamura, Y. Itikawa and N. Itoh, *Institute of Plasma Physics Report* IPPJ-AM-26, Nagoya University (1983).